Inorg. Chem. **2007**, *46*, 6613–6620

Penta- and Hexaruthenium Carbonyl 'Raft' Complexes Supported by Monocarborane Cage Ligands

Shaowu Du, Bruce E. Hodson, Peng Lei, Thomas D. McGrath, and F. Gordon A. Stone*

Department of Chemistry and Biochemistry, Baylor University, Waco, Texas 76798-7348

Received April 19, 2007

Reaction between $[PPh_4][closo\text{-}4\text{-}CB_8H_9]$ and $[Ru_3(CO)_{12}]$ in refluxing toluene affords the unprecedented hexaruthenium metallacarborane salt $[PPh_4][2,3,7\text{-}\{Ru(CO)_3\}\text{-}2,6,11\text{-}\{Ru(CO)_3\}\text{-}7,11,12\text{-}\{Ru(CO)_3\}\text{-}3,6,12\text{-}(\mu\text{-}H)_3\text{-}2,2,7,7,11,11\text{-}(CO)_6\text{-}closo\text{-}2,7,11,1\text{-}Ru_3CB_8H_6]$ (**1a**), which contains a planar Ru_6 'raft' supported by a $\{CB_8\}$ monocarborane cluster. Addition of $[CuCl(PPh_3)]_4$ and $Tl[PF_6]$ to a CH_2Cl_2 solution of **1a** results in simple cation replacement, forming the analogous $[Cu(PPh_3)_3]^+$ salt (**1b**). The phenyl-substituted monocarborane $[NEt_4][6\text{-}Ph\text{-}nido\text{-}6\text{-}CB_9H_{11}]$ reacts with $[Ru_3(CO)_{12}]$ in refluxing 1,2-dimethoxyethane to afford the pentaruthenium cluster species $[N(PPh_3)_2]\text{-}[2,3,7\text{-}\{Ru(CO)_3\}\text{-}3,4,8\text{-}\{Ru(CO)_3\}\text{-}7,8\text{-}(\mu\text{-}H)_2\text{-}1\text{-}Ph\text{-}2,2,3,3,4,4\text{-}(CO)_6\text{-}hypercloso\text{-}2,3,4,1\text{-}Ru_3CB_8H_6]$ (**2**), after addition of $[N(PPh_3)_2]Cl$. Treatment of **2** with $[CuCl(PPh_3)]_4$ and $Tl[PF_6]$ in CH_2Cl_2 forms the zwitterionic complex $[10,12\text{-}\{exo\text{-}Cu(PPh_3)_2\}\text{-}2,3,7\text{-}\{Ru(CO)_3\}\text{-}3,4,8\text{-}\{Ru(CO)_3\}\text{-}7,8,10,12\text{-}(\mu\text{-}H)_4\text{-}1\text{-}Ph\text{-}2,2,3,3,4,4\text{-}(CO)_6\text{-}hypercloso\text{-}2,3,4,1\text{-}Ru_3\text{-}CB_8H_4]$ (**3**). Substitution of CO by PPh_3 with concomitant cation replacement occurs on introduction of $[AuCl(PPh_3)]$, $Tl[PF_6]$, and PPh_3 to a CH_2Cl_2 solution of **2**, forming $[Au(PPh_3)_2][2,3,7\text{-}\{Ru(CO)_2PPh_3\}\text{-}3,4,8\text{-}\{Ru(CO)_2PPh_3\}\text{-}7,8\text{-}(\mu\text{-}H)_2\text{-}1\text{-}Ph\text{-}2,2,3,3,4,4\text{-}(CO)_6\text{-}hypercloso\text{-}2,3,4,1\text{-}Ru_3CB_8H_6]$ (**4**). Crystallographic studies confirmed the cluster architectures in **1b**, **2**, and **3**.

Introduction

For decades polyhedral heteroboranes have been a bountiful area of research for cluster chemists.[1] Their study led to the formulation of the Wade−Williams relationship, which associates the geometry of cluster species with the number of skeletal electrons available for cluster bonding.[2] More recently, a number of compounds have been characterized with seemingly erroneous architectures for their Wade−Williams electron counts.[3] A new hypercloso cluster class was recognized having two fewer skeletal electrons in comparison with the analogous closo species.[4]

Examples of the hypercloso architecture in metalla(car)borane complexes containing rhenium,[5a] rhodium,[5a] iridium,[5b] manganese,[5c] platinum,[5c] tungsten,[5d] and ruthenium[5a,6] are known. The last includes $[1\text{-}(\eta^6\text{-}C_6Me_6)\text{-}hypercloso\text{-}1\text{-}RuB_9H_9]$, which demonstrates the electronic difference between hypercloso and closo structures by undergoing a reversible two-electron reduction, forming $[2\text{-}(\eta^6\text{-}C_6Me_6)\text{-}closo\text{-}2\text{-}RuB_9H_9]^{2-}$.[5a] Other ruthena(car)borane complexes are known to exhibit similar structural abnormalities.[6c] The flexibility of electron donation by the ruthenium vertex in each case is presumed to play a key role in allowing the structural motifs observed.

* To whom correspondence should be addressed. E-mail: gordon_stone@baylor.edu.

(1) (a) Vyakaranam, K.; Maguire, J. A.; Hosmane, N. S. *J. Organomet. Chem.* **2002**, *646*, 21. (b) Weller, A. S. *Spec. Period. Rep. Organomet. Chem.* **2001**, *29*, 115. (c) Stíbr, B. *Chem. Rev.* **1992**, *92*, 225 and articles cited therein.

(2) (a) Williams, R. E. *Inorg. Chem.* **1971**, *10*, 210. (b) Wade, K. *J. Chem. Soc., Chem. Commun.* **1971**, 792. Mingos, D. M. P. *Nature (London), Phys. Sci.* **1972**, *236*, 99. (c) Rudolph, R. W. *Acc. Chem. Res.* **1976**, *9*, 446. (d) Mason, R.; Thomas, K. M.; Mingos, D. M. P. *J. Am. Chem. Soc.* **1973**, *6*, 3802.

(3) (a) Greenwood, N. N. *Pure Appl. Chem.* **1983**, *55*, 77. (b) Bould, J.; Greenwood, N. N.; McDonald, W. S. *J. Chem. Soc., Chem. Commun.* **1982**, 465. (c) Bould, J.; Crook, J. E.; Greenwood, N. N.; Kennedy, J. D.; McDonald, W. S. *J. Chem. Soc., Chem. Commun.* **1982**, 346.

(4) Baker, R. T. *Inorg. Chem.* **1986**, *25*, 109.

(5) (a) Littger, R.; Englich, U.; Ruhlandt, S.; Spencer, J. T. *Angew. Chem., Int. Ed.* **2000**, *39*, 1472. (b) Ditzel, E. J.; Fontaine, X. L. R.; Greenwood, N. N.; Kennedy, J. D.; Thornton-Pett, M. *J. Chem. Soc., Chem. Commun.* **1989**, 1262. (c) Du, S.; Jeffery, J. C.; Kautz, J. A.; Lu, X. L.; McGrath, T. D.; Miller, T. A.; Riis-Johannessen, T.; Stone, F. G. A. *Inorg. Chem.* **2005**, *44*, 2815. (d) Carr, N.; Mullica, D. F.; Sappenfield, E. L.; Stone, F. G. A. *Organometallics* **1992**, *11*, 3697.

(6) (a) Pisareva, I. V.; Konoplev, V. E.; Petrovskii, P. V.; Vorontsov, E. V.; Dolgushin, F. M.; Yanovsky, A. I.; Chizhevsky, I. T. *Inorg. Chem.* **2004**, *43*, 6228. (b) Pisareva, I. V.; Chizhevsky, I. T.; Petrovskii, P. V.; Bregadze, V. I.; Dolgushin, F. M.; Yanovsky, A. I. *Organometallics* **1997**, *16*, 5598. (c) Bown, M.; Fontaine, X. L. R.; Greenwood, N. N.; Kennedy, J. D.; MacKinnon, P. *J. Chem. Soc., Chem. Commun.* **1987**, 817.

10.1021/ic700746j CCC: $37.00
Published on Web 06/30/2007

Chart 1

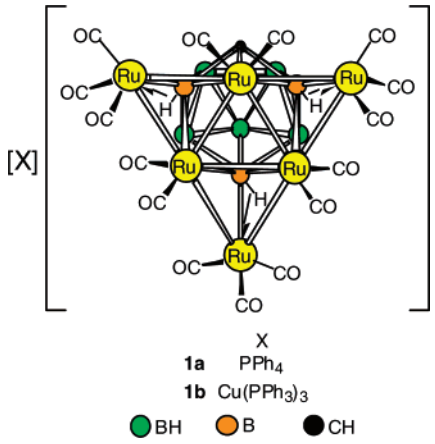

Metallacarboranes reported in the literature are generally those with 12-vertex icosahedral architectures, derived from 11-vertex [*nido*-$C_nB_mH_{11}]^{x-}$ ($n = 1, 2$; $m = 10, 9$; $x = 3, 2$) 'carbollide' anions.[7] We have been investigating transition metal complexes incorporating the relatively under-represented 7−10-vertex *mono*carborane clusters. To date, complexes containing these smaller cages have been prepared with a variety of transition metal atoms,[7,8] though such species are still by no means numerous. A proven synthetic strategy in this area is the thermally induced oxidative insertion of zerovalent metal carbonyl fragments into closo monocarboranes.[9] Herein we extend this methodology to include the use of {$Ru(CO)_3$} moieties derived from [$Ru_3(CO)_{12}$].

We are unaware of any ruthena(car)borane complexes containing more than three Ru atoms, either intra or extra to the cluster core, despite high-homonuclearity ruthenium carbonyl complexes with a range of multidentate ligands having been reported in the literature for decades.[10] However, we now describe a propensity for the formation of penta- and hexaruthenacarborane clusters using {CB_n} ($n = 8, 9$) monocarborane cage substrates. The polyruthenium 'raft' moieties formed contribute to closed 12-vertex {Ru_3CB_8} clusters with, in some cases, hypercloso geometries.

Results and Discussion

The formation of the hexaruthenium carborane complex [PPh_4][2,3,7-{$Ru(CO)_3$}-2,6,11-{$Ru(CO)_3$}-7,11,12-{$Ru(CO)_3$}-3,6,12-(μ-H)$_3$-2,2,7,7,11,11-$(CO)_6$-*closo*-2,7,11,1-$Ru_3CB_8H_6$] (**1a**) (Chart 1) proceeds via reaction between [$Ru_3(CO)_{12}$] and [PPh_4][*closo*-4-CB_8H_9] in toluene at reflux temperatures. Physical and spectroscopic data for **1a** are detailed in Tables 1−3. Several X-ray diffraction studies on crystals of **1a** only allowed for the formulation of a heavy atom structure. For this reason, **1a** was treated with a source of {$Cu(PPh_3)$}$^+$, in the expectation of forming a neutral, zwitterionic compound, possibly more amenable to crystallographic determination. However, the reaction merely afforded the analogous [$Cu(PPh_3)_3$]$^+$ salt (**1b**) via straightforward cation metathesis. An X-ray crystallographic study of **1b** established the structure for the anion shown in Figure 1 which, in conjunction with IR and NMR spectroscopic data, showed it to be identical to the anion of **1a**.

Table 1. Analytical and Physical Data

compd	color	yield %	ν_{max}(CO)[a]/cm^{-1}	anal. %[b] C	anal. %[b] H
1a	dark green	30	2085s, 2054vs, 2015s, 2001s	35.5 (35.3)[c]	2.8 (2.7)
1b	dark green	76	2085s, 2056vs, 2016s, 2000s	42.5 (42.4)	2.7 (2.7)
2	violet	33	2079s, 2057vs, 2020vs, 2004vs, 1956m	43.8 (43.5)[d]	3.1 (2.9)
3	violet	86	2083s, 2062vs, 2026vs, 2010vs, 1963m	41.5 (41.0)	3.0 (2.7)
4	dark green	73	2028s, 2006vs, 1980s, 1961s, 1932m	48.6 (48.3)	3.8 (3.3)

[a] Measured in CH_2Cl_2; a broad, medium-intensity band observed at ca. 2500−2550 cm^{-1} in the spectra of all compounds is due to B−H absorptions. [b] Calculated values are given in parentheses. In addition, %N for **2** = 0.9 (0.9). [c] Co-crystallizes with 2.5 molar equiv of acetone. [d] Co-crystallizes with 0.5 molar equiv of C_6H_6.

An essentially planar {Ru_6} triangular raft species is shown, ligated by a formally {*hypho*-CB_8H_9}$^{7-}$ monocarborane fragment centered over one 'face' of the raft and 15 carbonyl groups occupying the remaining Ru atom coordination sites. The three central Ru atoms of the Ru_6 moiety [Ru(2), Ru(7), and Ru(11), as shown in Figure 1 for the anion of **1b**] and the associated {CB_8} unit together constitute a 12-vertex {Ru_3CB_8} pseudo-icosahedron having a closo ($n + 1$, where n is the number of vertices) skeletal electron pair count, in compliance with the Wade−Williams relationship.[2] The remaining exo-polyhedral {$Ru(CO)_3$} moieties cap three individual {Ru_2B} trigonal faces of the cluster, supported by two direct Ru−Ru bonds and a 3-center, 2-electron B−H ⇀ Ru interaction in each case.

Alternatively, the formally {*hypho*-CB_8H_9}$^{7-}$ carborane fragment can be considered a 12-electron donor ($6\pi + 6$ from 3 × B−H ⇀ Ru agostic) to the {Ru_6} triangular raft, which hence attains a 90 valence-electron count as predicted by simple EAN (effective atomic number) rules. The {Ru_6} moiety is oriented with respect to the open face of the carborane cluster such that a B−H ⇀ Ru agostic bond to each of the three exopolyhedral {$Ru(CO)_3$} units is achieved. This disposition is imposed by the relatively acidic proton of the cage {CH} unit being unable to engage in a C−H ⇀ Ru interaction.

A speculative pathway of formation for the ruthenium raft present in **1a** is depicted in Scheme 1. Initial 'redox condensation' of [$Ru_3(CO)_{12}$] molecules could form an

(7) (a) Grimes, R. N. In *Comprehensive Organometallic Chemistry*; Wilkinson, G., Abel, E. W., Stone, F. G. A., Eds.; Pergamon Press: Oxford, 1982; Vol. 1, Section 5.5. (b) Grimes, R. N. In *Comprehensive Organometallic Chemistry II*; Abel, E. W., Stone, F. G. A., Wilkinson, G., Eds.; Pergamon Press: Oxford, 1995; Vol. 1, Chapter 9. (c) Grimes, R. N. *Coord. Chem. Rev.* **2000**, *200*−*202*, 773.
(8) McGrath, T. D.; Stone, F. G. A. *Adv. Organomet. Chem.* **2005**, *53*, 1.
(9) For example: (a) Franken, A.; McGrath, T. D.; Stone, F. G. A. *Organometallics* **2005**, *24*, 5157. (b) Lu, X. L.; McGrath, T. D.; Stone, F. G. A. *Organometallics* **2006**, *25*, 2590. (c) Franken, A.; McGrath, T. D.; Stone, F. G. A. *Inorg. Chem.* **2006**, *45*, 2669. (d) Franken, A.; Lei, P.; McGrath, T. D.; Stone, F. G. A. *Chem. Commun.* **2006**, 3423.
(10) Shriver, D. F.; Kaesz, H. D.; Adams, R. D. In *The Chemistry of Metal Cluster Complexes*; VCH: New York, 1990.

Table 2. ^{1}H and ^{13}C NMR Data[a]

compd	$^{1}H/\delta$ [b]	$^{13}C/\delta$ [c]
1a	8.00−7.64 (m, 20H, Ph), 3.67 (br s, 1H, cage CH), *ca.* −9.6 (br, 3H, B−H ⇀ Ru)	214.8, 211.5, 208.8, 208.4, 188.6 (br) (CO), 135.8−118.0 (Ph), 19.3 (br, cage C)
1b	7.48−7.07 (m, 45H, Ph), 3.70 (br s, 1H, cage CH), *ca.* −9.6 (br, 3H, B−H ⇀ Ru)	214.8, 211.6, 208.9, 208.4, 188.5 (br) (CO), 134.8−128.1 (Ph), 19.2 (br, cage C)
2	7.63 (m, 2H, cage Ph), 7.57−7.33 (m, 30H, PPh), 7.10 (m, 2H, cage Ph), 7.06 (m, 1H, cage Ph), *ca.* −5.3 (br, 2H, B−H ⇀ Ru)	217.8, 206.7, 202.9, 199.2 (br), 196.0, 188.1 (br), 187.0 (br) (CO), 206.0 (br, cage C), 158.0 (cage-C_6H_5 (*ipso*)), 134.0−126.0 (Ph)
3	7.78 (m, 2H, cage Ph), 7.63−7.30 (m, 30H, PPh), 7.15 (m, 2H, cage Ph), 7.14 (m, 1H, cage Ph), *ca.* −5.5 (br, 2H, B−H ⇀ Ru)	216.2, 205.5, 201.5, 198.2 (br), 195.3, 187.3 (br), 186.6 (CO), 204.7 (br, cage C), 157.1 (cage-C_6H_5 (*ipso*)), 134.1−126.9 (Ph)
4	7.67 (m, 2H, cage Ph), 7.59−7.28 (m, 60H, PPh), 7.28 (m, 2H, cage Ph), 7.06 (m, 1H, cage Ph), *ca.* −4.4 (br, 2H, B−H ⇀ Ru)	222.9, 212.5 (d, J(PC) = 10), 209.9, 204.9, 199.7, 194.1 (br d, J(PC) = 16), 193.7 (br, cage C), 159.1 (cage-C_6H_5 (*ipso*)), 133.8−122.6 (Ph)

[a] Chemical shifts (δ) in ppm, coupling constants (J) in Hz; measurements at ambient temperatures in CD_2Cl_2. [b] Resonances for terminal BH protons occur as broad, unresolved signals in the range δ ca. −1 to +3. [c] ^{1}H-decoupled chemical shifts are positive to high frequency of $SiMe_4$.

Table 3. ^{11}B and ^{31}P NMR Data[a]

compd	$^{11}B/\delta$ [b]	$^{31}P/\delta$ [c]
1a	51.7, 40.4 (2B), −5.7 (3B), −10.0 (2B)	23.5
1b	51.5, 40.5 (2B), −5.7 (3B), −10.0 (2B)	1.7 (br)
2	55.5 (2B), 18.0 (2B), 8.8 (2B), 4.9, −8.6	21.2
3	52.8 (2B), 15.7 (2B), 6.6 (2B), −0.4, −12.9	0.8 (br)
4	53.8 (2B), 16.6 (2B), 8.8 (2B), 2.3, −8.4	44.0 (Au−P), 43.8 (Ru−P)

[a] Chemical shifts (δ) in ppm; measurements at ambient temperatures in CD_2Cl_2. [b] ^{1}H-decoupled chemical shifts are positive to high frequency of $BF_3{\cdot}Et_2O$ (external); resonances are of unit integral except where indicated. [c] ^{1}H-decoupled chemical shifts are positive to high frequency of 85% H_3PO_4 (external).

octahedral {Ru_6} fragment (**A**),[11] which on six-electron reduction by the carborane cage (breaking three Ru−Ru cluster bonds) forms the planar trigonal raft geometry (**B**). Similar mechanisms have been proposed for the formation of a related osmium species,[12a] and for an {Ru_5} cluster[12b] similar to compound **2** (described below).

Spectroscopic data for **1a** are consistent with the formulation given, specifically with the structure established for the anion of the analogous salt **1b**. Strong stretching bands for the 15 CO groups are observed in the IR spectrum of **1a** at 2085, 2054, 2015, and 2001 cm^{-1}. A $^{11}B\{^{1}H\}$ NMR study of **1a** revealed four peaks in the intensity ratio 1:2:3(2 + 1 coincidence):2, indicating that the C_s molecular symmetry of the anion is maintained in solution. Accordingly, nine separate resonances for the CO groups would be expected in the $^{13}C\{^{1}H\}$ NMR spectrum. However, only five peaks are observed, appearing at δ 214.8, 211.5, 208.8, 208.4, and 188.6 (br), a discrepancy attributed to coincidence. In addition to those described for the CO groups, a broad peak at δ 19.3 assigned to the cage {CH} vertex appeared therein. The ^{1}H NMR spectrum of **1a** contained broad peaks due to the cage {CH} vertex (δ 3.67) and to the three B−H ⇀ Ru agostic interactions (an unresolved quartet centered on δ −9.6). Given that only two of these agostic interactions are expected to be electronically equivalent, this resonance is assigned as a (2 + 1) coincidence. Data typical for a $[PPh_4]^+$ counterion were observed in the relevant NMR spectra.

Previously, addition of suitable monocationic transition metal fragments to anionic metallacarborane clusters has led to the formation of neutral zwitterionic, rather than anionic, complexes. Direct metal-to-metal bonding interactions supported by B−H ⇀ M agostic bridges often result.[13] However, as noted above, addition of $\{Cu(PPh_3)\}^+$ (formed in situ from $[CuCl(PPh_3)]_4$ and $Tl[PF_6]$) to **1a** merely afforded cation exchange, giving **1b** (Chart 1). Physical and spectroscopic data for **1b** are listed in Tables 1−3 and confirm the anionic fragment therein to be identical to that found in **1a**. The $\{Cu(PPh_3)_3\}^+$ cation in the former is revealed in the $^{31}P\{^{1}H\}$ NMR spectrum as a broad peak at δ 1.7. Characteristic signals due to the phenyl rings are present in the $^{13}C\{^{1}H\}$ and ^{1}H NMR spectra (Table 2). A related process was observed on addition of PPh_3 to the zwitterionic species [2,2-$(CO)_2$-7-(μ-H)-11-μ-{$Au(PPh_3)$}-7,11-{$Ru_2(\mu$-H)$(CO)_6$}-*closo*-2,1-$RuCB_{10}H_8$], forming the salt $[Au(PPh_3)_2]$[2,2-$(CO)_2$-7,11-(μ-H)$_2$-7,11-{$Ru_2(CO)_6$}-*closo*-2,1-$RuCB_{10}H_8$].[14]

Only a handful of compounds having the essentially planar (average angle of declination of the three 'wingtip' ruthenium triangles from the central Ru(2)Ru(7)Ru(11) plane being only 1.3° in **1b**) {M_6} geometry exhibited by the anion of **1a** and **1b** are known, and they are restricted to ruthenium[15] and osmium[12a,16] species. A lengthening of Ru−Ru distances in the central Ru_3 triangle of the raft has been noted in these compounds and is presumed to be as a result of electron donation by peripheral ligands into an antibonding MO on the metal cluster.[15b] No such effect is apparent in **1b**, all nine Ru−Ru connectivities being in the range 2.75−2.80 Å.

In contrast to the formation of **1a**, treatment of the 10-vertex carborane salt $[NEt_4]$[6-Ph-*nido*-6-CB_9H_{11}] with [$Ru_3(CO)_{12}$] in refluxing DME (1,2-dimethoxyethane) afforded the pentaruthenacarborane $[N(PPh_3)_2]$[2,3,7-{$Ru(CO)_3$}-3,4,8-{$Ru(CO)_3$}-7,8-(μ-H)$_2$-1-Ph-2,2,3,3,4,4-$(CO)_6$-*hypercloso*-

(11) Hayward, C.-M. T.; Shapley, J. R. *Inorg. Chem.* **1982**, *21*, 3816.
(12) (a) Goudsmit, R. J.; Johnson, B. F. G.; Lewis, J.; Raithby, P. R.; Whitmire, K. H. *J. Chem. Soc., Chem. Commun.* **1982**, 640. (b) Bruce, M. I.; Matisons, J. G.; Rodgers, J. R.; Wallis, R. C. *J. Chem. Soc., Chem. Commun.* **1981**, 1070.
(13) Jelliss, P. A.; Stone, F. G. A. *J. Organomet. Chem.* **1995**, *500*, 307.
(14) Ellis, D. D.; Franken, A.; Stone, F. G. A. *Organometallics* **1999**, *18*, 2362.
(15) Examples include: (a) Bhaduri, S.; Sharma, K.; Jones, P. G. *J. Chem. Soc., Chem. Commun.* **1987**, 1769. (b) Bhaduri, S.; Sharma, K.; Khwaja, H.; Jones, P. G. *J. Organomet. Chem.* **1991**, *412*, 169. (c) Brandl, M.; Brunner, H.; Cattey, H.; Mugnier, Y.; Wachter, J.; Zabel, M. *J. Organomet. Chem.* **2002**, *659*, 22.
(16) For example: Goudsmit, R. J.; Johnson, B. F. G.; Lewis, J.; Raithby, P. R.; Whitmire, K. H. *J. Chem. Soc., Chem. Commun.* **1983**, 246.

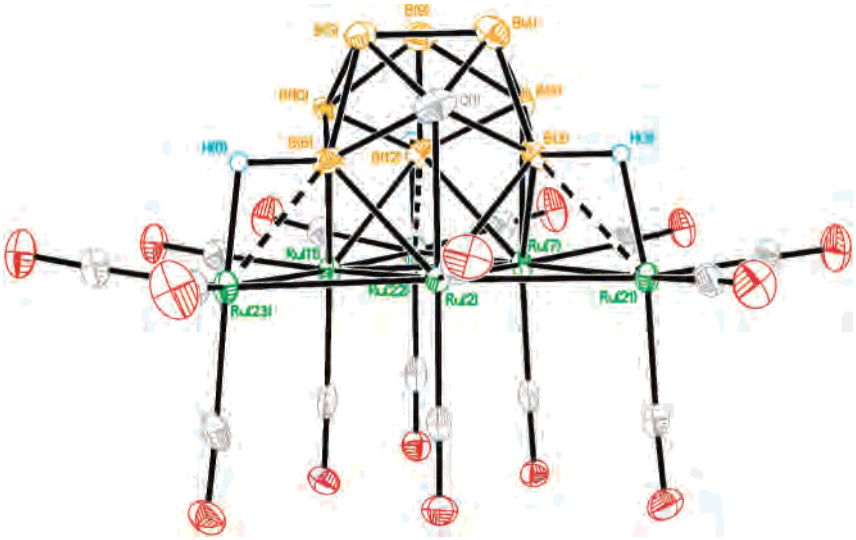

Figure 1. Structure of the anion of **1b** showing the crystallographic labeling scheme. In this and subsequent figures, thermal ellipsoids are drawn with 40% probability, and only chemically significant H atoms are shown. Selected distances (Å) are as follows. Ru(2)−C(1) 2.302(8), B(3)−Ru(2) 2.260(7), B(3)−Ru(21) 2.278(8), B(3)−Ru(7) 2.295(7), B(6)−Ru(2) 2.245(8), B(6)−Ru(23) 2.265(8), B(6)−Ru(11) 2.309(8), B(8)−Ru(7) 2.317(8), B(10)−Ru(11) 2.295(7), B(12)−Ru(7) 2.250(7), B(12)−Ru(11) 2.267(8), B(12)−Ru(22) 2.270(8), Ru(2)−Ru(7) 2.7701(7), Ru(2)−Ru(11) 2.7720(7), Ru(2)−Ru(21) 2.7911(8), Ru(2)−Ru(23) 2.7987(8), Ru(7)−Ru(11) 2.7460(8), Ru(7)−Ru(21) 2.7739(7), Ru(7)−Ru(22) 2.7879(7), Ru(11)−Ru(23) 2.7643(8), Ru(11)−Ru(22) 2.7788(7), Ru(21)−H(3) 1.69(6), Ru(22)−H(12) 1.78(7), Ru(23)−H(6) 1.65(6).

Scheme 1. Three Successive Two Electron Reductions of an Octahedral Cluster, Arbitrarily Breaking Bonds 2−6, 2−3, and 3−6 to Form a Triangular 'Raft' Geometry

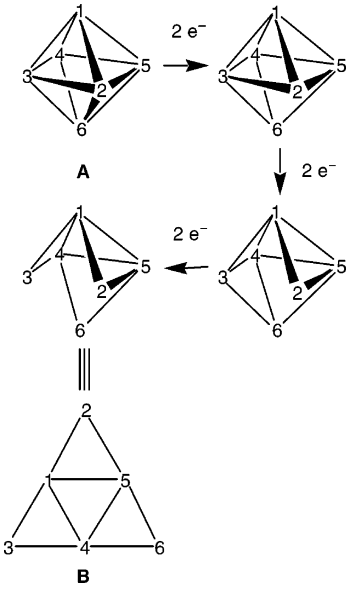

Chart 2

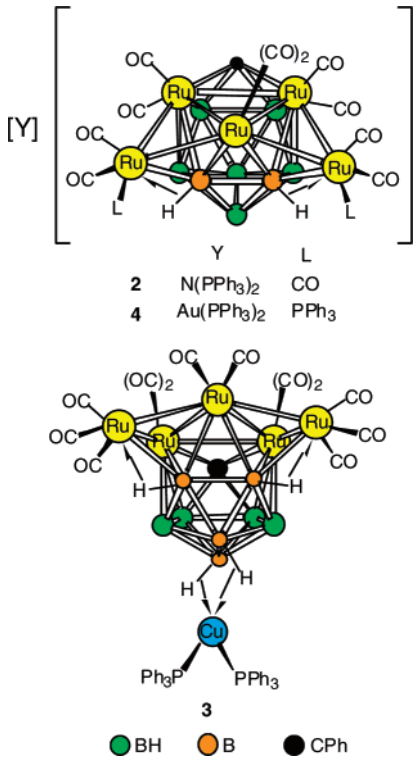

2,3,4,1-$Ru_3CB_8H_6$] (**2**) after addition of $[N(PPh_3)_2]Cl$ (Chart 2). Physical and spectroscopic data for **2** are given in Tables 1−3. A crystallographic determination of **2** defined the structure for the anion to be that shown in Figure 2. The $\{Ru_5\}$ unit adopts bi-edge-bridged triangular geometry, few examples of which are known.[12b,17] One {BH} vertex has been lost from the [6-Ph-*nido*-6-CB_9H_{11}]$^-$ starting material, affording a $\{CB_8\}$ fragment, which in conjunction with the three 'central' Ru atoms (Ru(2), Ru(3), and Ru(4)) of the $\{Ru_5\}$ moiety, constitutes a 12-vertex $\{Ru_3CB_8\}$ cluster. An exo-polyhedral $\{Ru(CO)_3\}$ fragment caps both the Ru(2)-Ru(3)B(7) and Ru(3)Ru(4)B(8) trigonal faces, ligated via two direct Ru−Ru bonds and a B−H ⇀ Ru 3-center, 2-electron agostic interaction in each case. The formation of the $\{Ru_5\}$ raft in **2**, in preference to the $\{Ru_6\}$ configuration observed in the anions of **1a** and **1b**, is tentatively associated with the deboronation of the [6-Ph-*nido*-6-CB_9H_{11}]$^-$ starting material.

(17) Examples include: (a) MacLaughlin, S. A.; Taylor, N. J.; Carty, A. J. *Organometallics* **1983**, *2*, 1194. (b) MacLaughlin, S. A.; Taylor, N. J.; Carty, A. J. *Organometallics* **1984**, *3*, 392. (c) Bruce, M. I.; Williams, M. L.; Patrick, J. M.; White, A. H. *J. Chem. Soc., Dalton Trans.* **1985**, 1229. (d) Davies, J. E.; Nahar, S.; Raithby, P. R.; Shields, G. P. *J. Chem. Soc., Dalton Trans.* **1997**, 13. (e) Bruce, M. I.; Schulz, M.; Skelton, B. W.; White, A. H. *J. Cluster Sci.* **2000**, *11*, 79.

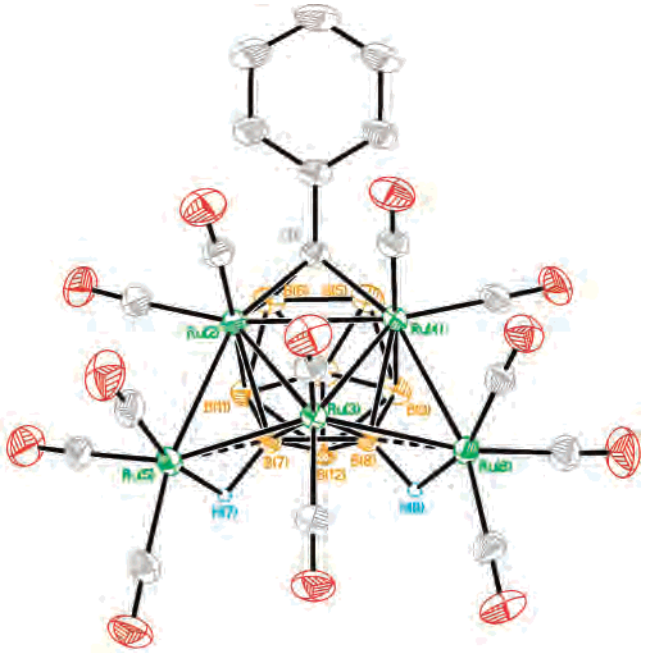

Figure 2. Structure of the anion of **2** showing the crystallographic labeling scheme. Selected distances (Å) are as follows. Ru(2)−C(1) 2.175(2), Ru(4)−C(1) 2.174(2), B(5)−C(1) 1.660(3), B(6)−C(1) 1.657(3), B(5)−Ru(4) 2.283(3), B(6)−Ru(2) 2.289(3), B(7)−Ru(2) 2.247(2), B(7)−Ru(3), 2.292(2), B(7)−Ru(5) 2.298(2), B(8)−Ru(4) 2.243(2), B(8)−Ru(3) 2.300(2), B(8)−Ru(6) 2.319(2), B(9)−Ru(4) 2.331(2), B(11)−Ru(2) 2.328(3), Ru(2)−Ru(3) 2.7531(3), Ru(2)−Ru(4) 2.8767(3), Ru(2)−Ru(5) 2.8785(3), Ru(3)−Ru(5) 2.7005(3), Ru(3)−Ru(6) 2.7305(3), Ru(3)−Ru(4) 2.7322(3), Ru(4)−Ru(6) 2.8429(3).

Chart 3

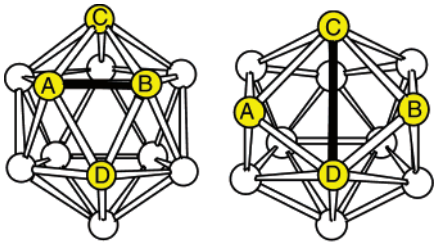

While the $\{Ru_3CB_8\}$ cluster core composition in **2** is identical to that found in **1a**, the connectivity pattern is consistent with a hypercloso rather than closo metallacarborane species. Hypercloso geometry in a 12-vertex species can be regarded (Chart 3) as a hypothetical breaking of the **A**−**B** connectivity in the closo compound, with formation of the perpendicular **C**−**D** connectivity, though it is not suggested that this process actually occurs. The hypercloso geometry contains the four-connected vertices **A** and **B** (corresponding to C(1) and Ru(3) in **2**) and the six-connected vertices **C** and **D** (corresponding to Ru(2) and Ru(4) in **2**), the remaining vertices being five-connected. Such species use *n* skeletal electron pairs for cluster bonding within a closed deltahedron (where *n* is the number of vertices),[4] though we have found that the presence of transition metal vertices, as well as the flexible electron contribution therefrom, can complicate skeletal electron counting.[5c] The 12-vertex $\{Ru_3CB_8\}$ moiety in **2** is two electrons short of the expected electron count for a closo cluster and subsequently has not adopted the expected pseudo-icosahedral geometry. We know of only one other example of a 12-vertex metallacarborane having hypercloso architecture, that being a $\{WC_2B_9\}$ species.[5d]

With 74 electrons, the Ru_5 raft moiety in **2** is formally two electrons short of the EAN prediction for a cluster containing seven M−M bonds, assuming the carborane cage to be a 10-electron ($6\pi + 4$ from 2 × B−H ⇀ Ru agostic) donor. The 'wingtip' ruthenium triangles {Ru(2)Ru(3)-Ru(5)} and {Ru(3)Ru(4)Ru(6)} are declined from the central Ru(2)Ru(3)Ru(4) plane by 21.3° and 19.3°, respectively, values comparable with previous examples of this architecture.[12b,17]

The formation of **2** might well proceed similarly to that of **1a** via a six-electron reduction of an octahedral $\{Ru_6\}$ fragment. However, this hypothetical complex is evidently disfavored and ejects one B and one Ru atom (and associated ligands) to form the observed $\{Ru_5\}$ unit with hypercloso geometry.

The orientation of the Ru_5 raft with respect to the open face of the carborane cluster is again influenced by the necessity for B−H ⇀ Ru agostic bonds to support exo-polyhedral $\{Ru(CO)_3\}$ fragments, the cage {CPh} unit being unable to participate in such an interaction. In addition to the hypercloso geometry, the system is severely distorted due to the large radii of the Ru atoms in comparison with those of the boron and carbon atom vertices; the four-connected C(1) vertex has average C−B and C−Ru cluster connectivities of 1.66 and 2.17 Å, respectively.

A $^{11}B\{^1H\}$ NMR study revealed five resonances in a 2:2:2:1:1 intensity ratio, indicating a mirror-symmetric cluster as observed in the solid state. The carbonyl groups in **2** were observed in the IR spectrum as strong stretching bands at 2079, 2057, 2020, 2004, and 1956 cm^{-1} and as seven resonances in the $^{13}C\{^1H\}$ NMR spectrum over the range δ 217.8−187.0. Hydrogen atoms involved in the B−H ⇀ Ru bridges were present in the corresponding ^1H NMR spectrum as a broad resonance at δ −5.3 having a relative intensity equal to two protons. Both spectra contained diagnostic signals for the cage {CPh} unit and the $[N(PPh_3)_2]^+$ counterion.

Introduction of $[CuCl(PPh_3)]_4$ and $Tl[PF_6]$ to a CH_2Cl_2 solution of **2** yielded the neutral, zwitterionic compound [10,-12-{*exo*-$Cu(PPh_3)_2$}-2,3,7-{$Ru(CO)_3$}-3,4,8-{$Ru(CO)_3$}-7,8,-10,12-(μ-H)$_4$-1-Ph-2,2,3,3,4,4-$(CO)_6$-*hypercloso*-2,3,4,1-$Ru_3CB_8H_4$] (**3**) (Chart 2), the molecular structure of which is shown in Figure 3. The C_s symmetry observed therein is retained in solution, as indicated by a 2:2:2:1:1 peak intensity ratio in the $^{11}B\{^1H\}$ NMR spectrum. A $\{Cu(PPh_3)_2\}^+$ moiety is bound exo-polyhedral to the central $\{Ru_3CB_8\}$ cluster surface via two B−H ⇀ Cu agostic interactions involving vertices BH(10) and BH(12). The absence of resonances due to the hydrogen atoms of these groups from the ^1H NMR spectrum is attributed to a rapid exchange of B−H binding sites on the NMR time scale, rendering any such peaks too broad to be observed.[18] The PPh_3 units give rise to a broad peak at δ 0.8 in the $^{31}P\{^1H\}$ NMR spectrum and to characteristic phenyl group resonances in the ^1H and ^{13}C-

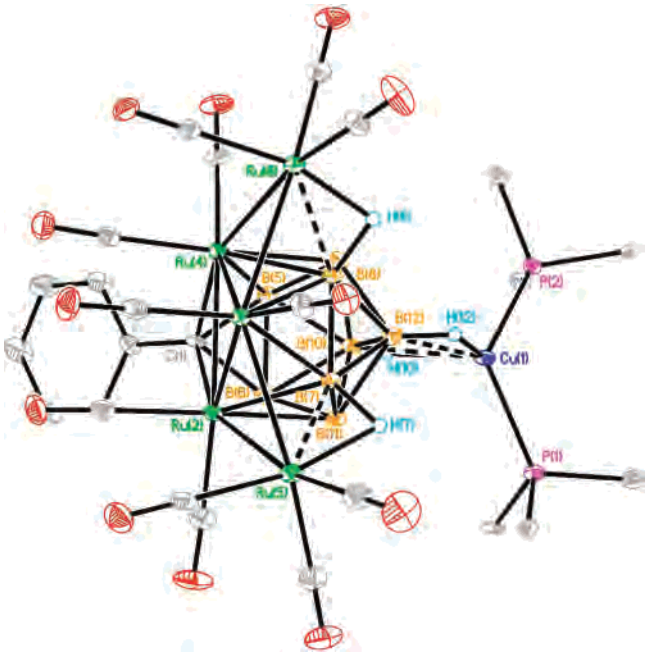

Figure 3. Structure of **3** showing the crystallographic labeling scheme. Only the ipso carbon atoms of phosphine phenyl rings are shown. Selected distances (Å) are as follows. B(5)−Ru(4) 2.248(4), B(6)−Ru(2) 2.250(4), B(7)−Ru(2) 2.222(4), B(7)−Ru(3) 2.239(4), B(7)−Ru(5) 2.257(4), B(8)−Ru(4) 2.210(4), B(8)−Ru(3) 2.250(4), B(8)−Ru(6) 2.272(4), B(9)−Ru(4) 2.275(4), B(11)−Ru(2) 2.278(4), B(10)−Cu(1) 2.433(4), B(12)−Cu(1) 2.376(4), Ru(2)−C(1) 2.140(4), Ru(2)−Ru(3) 2.7113(5), Ru(2)−Ru(4) 2.8226(5), Ru(2)−Ru(5) 2.8532(5), Ru(3)−Ru(6) 2.6631(5), Ru(3)−Ru(5) 2.6713(5), Ru(3)−Ru(4) 2.7278(5), Ru(4)−Ru(6) 2.8488(5), Ru(5)−H(7) 1.85(4), Ru(6)−H(8) 1.71(4).

{^{1}H} NMR spectra (Table 2). Carbonyl group resonances are present in the latter spectrum at δ 216.2, 205.5, 201.5, 198.2 (br), 195.3, 187.3 (br), and 186.6 (br), in addition to a broad peak at δ 204.7 due to the cage {CH} vertex. Hypercloso geometry is retained on formation of **3**, and indeed, the central {Ru_5CB_8} unit is essentially identical to that in **2**. On comparison, higher CO stretching frequencies for the carbonyl groups of **3** reflect the net neutral charge on the cluster versus analogous groups in the anion of **2** (Tables 1−3).

Whereas coordination of the {$Cu(PPh_3)_2$}$^+$ fragment to the cluster surface via B−H⇀Cu interactions was expected, the lack of formation of a direct Cu−Ru bond was not. Previously, anionic metallacarboranes have been used to great effect in the formation of polymetallic species containing direct metal−metal bonds;[8] a large number of such compounds have been prepared using the {$Cu(PPh_3)$}$^+$ synthon.[9a−c,19] The involvement of the {BH} vertices most distant from the carbon and ruthenium atoms within the cluster [BH(10) and BH(12)] intuitively suggests them to be of most hydridic character. The arrangement is presumably adopted as a result of the Ru vertices being sterically 'shielded' by carbonyl ligands, hence blocking attack by the {$Cu(PPh_3)_2$} fragment.

As for the reactions of compounds **1a** and **2** toward the {$Cu(PPh_3)$}$^+$ fragment, the behavior of the two ruthenacarboranes with the isolobal {$Au(PPh_3)$}$^+$ moiety is also different. Thus, **1a** gives no identifiable product, whereas reaction between **2** and {$Au(PPh_3)$}$^+$ (generated in situ from [$AuCl(PPh_3)$] and $Tl[PF_6]$) in the presence of PPh_3 affords cation replacement and substitution of two CO molecules by PPh_3, forming [$Au(PPh_3)_2$][2,3,7-{$Ru(CO)_2PPh_3$}-3,4,8-{$Ru(CO)_2PPh_3$}-7,8-(μ-H)$_2$-1-Ph-2,2,3,3,4,4-(CO)$_6$-*hypercloso*-2,3,4,1-$Ru_3CB_8H_6$] (**4**) (Chart 2). Details of an X-ray crystallographic study of **4** have been deposited as Supporting Information. Other than substitution by PPh_3 at each of the exo-polyhedral Ru atoms, the hypercloso {Ru_3CB_8} cluster core in **4** remains essentially identical to that in **2**, as confirmed on comparison of NMR spectroscopic data for the two compounds. Strong CO stretching bands appear at 2028, 2006, 1980, 1961, and 1932 cm^{-1} in the IR spectrum of **4**, values lower than those for **2** due to the presence of the relatively electron-donating phosphine ligands. A ^{31}P-{^{1}H} NMR study of **4** revealed a peak at δ 44.0 due to the [$Au(PPh_3)_2$]$^+$ cation, a value comparable with data previously reported for two-coordinate Au compounds.[20] Also present was a sharp peak at δ 43.8, assigned to the phosphorus atoms of the two Ru-bound PPh_3 units. The carborane moiety in **4** gave rise to five peaks of relative intensity 2:2:2:1:1 in a ^{11}B{^{1}H} NMR study; chemical shift values were almost identical to those in the analogous study of **2**, as expected given the close structural relationship between the two compounds.

Conclusion

The preparation of unusual polyruthenium raft species supported by monocarborane clusters has been demonstrated. Use of either {CB_9} or {CB_8} starting materials affords {Ru_5CB_8} or {Ru_6CB_8} compounds, respectively. Each of the compounds contains a different type of closed {Ru_3CB_8} core and, as such, is a rare example of a 12-vertex metallacarborane cluster containing three transition metal vertices. Moreover, in the pentaruthenium species, this {Ru_3CB_8} core has the unusual hypercloso geometry. Preliminary reactivity studies of this species provided the neutral, zwitterionic compound **3** and the phosphine-substituted species **4**, both also having a hypercloso geometry.

Experimental Section

Syntheses. All reactions were performed under an atmosphere of dry, oxygen-free dinitrogen using standard Schlenk-line techniques. Solvents were stored over and freshly distilled from appropriate drying agents prior to use. Petroleum ether refers to that fraction of boiling point 40−60 °C. Chromatography columns (typically ca. 15 cm in length and ca. 2 cm in diameter) were packed with silica gel (Acros, 60−200 mesh). Filtration through Celite

(18) (a) Cabioch, J.-L.; Dosset, S. J.; Hart, I. J.; Pilotti, M. U.; Stone, F. G. A. *J. Chem. Soc., Dalton Trans.* **1991**, 519. (b) Batten, S. A.; Jeffrey, J. C.; Jones, P. L.; Mullica, D. F.; Rudd, M. D.; Sappenfield, E. L.; Stone, F. G. A.; Wolf, A. *Inorg. Chem.* **1997**, *36*, 2570. (c) Ellis, D. D.; Franken, A.; Jelliss, P. A.; Kautz, J. A.; Stone, F. G. A.; Yu, P.-Y. *J. Chem. Soc., Dalton Trans.* **2000**, 2509.

(19) Hodson, B. E.; McGrath, T. D.; Stone, F. G. A. *Organometallics* **2005**, *24*, 3386.

(20) (a) Carriedo, G. A.; Howard, J. A. K.; Stone, F. G. A.; Went, M. J. *J. Chem. Soc., Dalton Trans.* **1984**, 2545. (b) Wynd, A. J.; Welch, A. J. *J. Chem. Soc., Chem. Commun.* **1987**, 1174. (c) Du, S.; Kautz, J. A.; McGrath, T. D.; Stone, F. G. A. *Inorg. Chem.* **2001**, *40*, 6563.

Table 4. Crystallographic Data for Compounds **1b**, **2**, and **3**

	1b·2CH_2Cl_2	**2**·0.5C_6H_6	**3**
formula	$C_{72}H_{58}B_8Cl_4CuO_{15}P_3Ru_6$	$C_{58}H_{46}B_8NO_{12}P_2Ru_5$	$C_{55}H_{43}B_8CuO_{12}P_2Ru_5$
fw	2154.33	1602.73	1613.20
cryst syst	monoclinic	triclinic	triclinic
space group	$P2_1/n$	$P\bar{1}$	$P\bar{1}$
a, Å	22.046(2)	11.1475(9)	12.0923(9)
b, Å	16.9959(16)	16.9338(17)	15.7652(13)
c, Å	23.643(2)	17.2434(16)	17.6006(14)
α, deg	90	79.248(2)	75.902(4)
β, deg	114.730(3)	89.604(3)	71.283(4)
γ, deg	90	83.781(2)	73.289(4)
V, Å^3	8046.5(13)	3178.8(5)	3001.0(4)
Z	4	2	2
wR2, R1 (all data)[a]	0.1504, 0.1041	0.0689, 0.0441	0.0811, 0.0586
wR2, R1 (obs[b] data)	0.1232, 0.0530	0.0643, 0.0279	0.0735, 0.0391
GOF[c]	1.027	1.065	1.049

[a] $wR2 = [\sum\{w (F_o^2 - F_c^2)^2\}/\sum w (F_o^2)^2]^{1/2}$; $R1 = \sum||F_o| - |F_c||/\sum|F_o|$. [b] $F_o > 4\sigma(F_o)$. [c] $GOF = [\sum\{w (F_o^2 - F_c^2)^2\}/(n - p)]^{1/2}$ where n = number of reflections and p = number of refined parameters.

typically employed a plug ca. 5 cm in length and 2 cm in diameter. NMR spectra were recorded at the following frequencies (MHz): ^{1}H, 360.1; ^{13}C, 90.6; ^{31}P, 145.8; and ^{11}B, 115.5. The reagents [NEt_4][6-Ph-*nido*-6-CB_9H_{11}],[21] [PPh_4][*closo*-4-CB_8H_9],[22] [$CuCl(PPh_3)]_4$,[23] and [$AuCl(PPh_3)$][24] were prepared according to literature methods.

Synthesis of [PPh_4][2,3,7-{$Ru(CO)_3$}-2,6,11-{$Ru(CO)_3$}-7,11,-12-{$Ru(CO)_3$}-3,6,12-(μ-H)$_3$-2,2,7,7,11,11-$(CO)_6$-*closo*-2,7,11,1-$Ru_3CB_8H_6$] (1a). A mixture of [PPh_4][*closo*-4-CB_8H_9] (0.45 g, 1.00 mmol) and [$Ru_3(CO)_{12}$] (1.41 g, 2.20 mmol) was heated in toluene (30 mL) at reflux temperatures for 12 h, after which all volatiles were removed in vacuo. The residue was extracted into CH_2Cl_2 (3 × ca. 10 mL portions), and the washings combined, filtered (Celite) and concentrated to ca. 5 mL, and transferred to the top of a chromatography column. Elution with CH_2Cl_2/petroleum ether (4:1) produced a dark green band, which was collected and reduced to dryness in vacuo to yield **1a** (0.43 g) as a dark green crystalline solid.

Synthesis of [Cu(PPh_3)$_3$][2,3,7-{$Ru(CO)_3$}-2,6,11-{$Ru(CO)_3$}-7,11,12-{$Ru(CO)_3$}-3,6,12-(μ-H)$_3$-2,2,7,7,11,11-$(CO)_6$-*closo*-2,7,-11,1-$Ru_3CB_8H_6$] (1b). To a CH_2Cl_2 (20 mL) solution of **1a** (0.15 g, 0.10 mmol) was added a mixture of [$CuCl(PPh_3)]_4$ (0.22 g, 0.15 mmol) and Tl[PF_6] (0.21 g, 0.60 mmol) with subsequent stirring at room temperature for 12 h. The resulting mixture was filtered (Celite), and the filtrate concentrated and transferred to the top of a chromatography column. Elution with CH_2Cl_2/petroleum ether (2:1) afforded a dark green fraction, which was collected and reduced to dryness in vacuo to yield **1b** (0.15 g) as a black crystalline solid.

Synthesis of [N(PPh_3)$_2$][2,3,7-{$Ru(CO)_3$}-3,4,8-{$Ru(CO)_3$}-7,8-(μ-H)$_2$-1-Ph-2,2,3,3,4,4-$(CO)_6$-*hypercloso*-2,3,4,1-$Ru_3CB_8H_6$] (2). A DME (30 mL) solution of [NEt_4][6-Ph-*nido*-6-CB_9H_{11}] (0.328 g, 1.00 mmol) and [$Ru_3(CO)_{12}$] (1.28 g, 2.00 mmol) was heated to reflux temperatures for 12 h. All volatiles were then removed in vacuo and a CH_2Cl_2 (20 mL) solution of [$N(PPh_3)_2$]Cl (0.537 g, 1.00 mmol) added. After being stirred for 2 h, the solution was filtered, concentrated to ca. 5 mL, and transferred to the top of a chromatography column. Elution with CH_2Cl_2/petroleum ether (3:1) afforded a violet band, which was collected and reduced to dryness in vacuo to yield **2** (0.512 g) as a dark violet crystalline solid.

Synthesis of [10,12-{*exo*-Cu(PPh_3)$_2$}-2,3,7-{$Ru(CO)_3$}-3,4,8-{$Ru(CO)_3$}-7,8,10,12-(μ-H)$_4$-1-Ph-2,2,3,3,4,4-$(CO)_6$-*hypercloso*-2,3,4,1-$Ru_3CB_8H_4$] (3). To a CH_2Cl_2 (20 mL) solution of **2** (0.15 g, 0.10 mmol) was added [$CuCl(PPh_3)]_4$ (0.22 g, 0.15 mmol) and Tl[PF_6] (0.21 g, 0.60 mmol) with subsequent stirring at room temperature for 12 h. The mixture was then filtered (Celite), and the filtrate was concentrated to ca. 5 mL in vacuo before being transferred to the top of a chromatography column. Elution using CH_2Cl_2/petroleum ether (2:1) afforded a violet fraction was, which was collected and reduced to dryness in vacuo to yield **3** (0.14 g) as a black crystalline solid.

Synthesis of [Au(PPh_3)$_2$][2,3,7-{$Ru(CO)_2PPh_3$}-3,4,8-{$Ru(CO)_2PPh_3$}-7,8-(μ-H)$_2$-1-Ph-2,2,3,3,4,4-$(CO)_6$-*hypercloso*-2,3,4,1-$Ru_3CB_8H_6$] (4). To a CH_2Cl_2 (20 mL) solution of **2** (0.15 g, 0.10 mmol) was added [$AuCl(PPh_3)$] (0.30 g, 0.60 mmol), Tl[PF_6] (0.21 g, 0.60 mmol), and PPh_3 (0.16 g, 0.60 mmol) with subsequent stirring at room temperature for 12 h. The mixture was then filtered (Celite), and the filtrate concentrated to ca. 5 mL before being transferred to the top of a chromatography column. Elution with CH_2Cl_2/petroleum ether (4:1) afforded a dark violet fraction, which was collected and reduced to dryness in vacuo to yield **4** (0.16 g) as a black crystalline solid.

X-ray Diffraction Experiments. Experimental data for compounds **1b**, **2**, and **3** are presented in Table 4. Diffraction data were acquired at 110(2) K using a Bruker-Nonius X8 Apex area-detector diffractometer (graphite-monochromated Mo Kα radiation, λ = 0.71073 Å). Several sets of data frames were collected at different θ values for various initial values of ϕ and ω, each frame covering a 0.5° increment of ϕ or ω. The data frames were integrated using SAINT;[25] the substantial redundancy in data allowed empirical absorption corrections (SADABS)[25] to be applied on the basis of multiple measurements of equivalent reflections.

The structures were solved (SHELXS-97)[26] via conventional direct methods and were refined (SHELXL-97) by full-matrix least-squares on all F^2 data using SHELXTL.[26] All non-hydrogen atoms were assigned anisotropic displacement parameters. The locations of the cage carbon atoms were verified by examination of the appropriate internuclear distances and the magnitudes of their isotropic thermal displacement parameters. All hydrogen atoms were set riding on their parent atoms in calculated positions with the

(21) (a) Brellochs, B. In *Contemporary Boron Chemistry*; Davidson, M. G., Hughes, A. K., Marder, T. B., Wade, K., Eds.; Royal Society of Chemistry: Cambridge, 2000; p 212. (b) Jelínek, T.; Thornton-Pett, M.; Kennedy, J. D. *Collect. Czech. Chem. Commun.* **2002**, *67*, 1035.
(22) Brellochs, B.; Backovsky, J.; Stíbr, B.; Jelínek, T.; Holub, J.; Bakardjiev, M.; Hnyk, D.; Hofmann, M.; Císarová, I.; Wrackmeyer, B. *Eur. J. Inorg. Chem.* **2004**, 3605.
(23) Jardine, F. H.; Rule, J.; Vohra, G. A. *J. Chem. Soc. A* **1970**, 238.
(24) Bruce, M. I.; Nicholson, B. K.; Bin Shawkataly, O. *Inorg. Synth.* **1989**, *26*, 325.
(25) *APEX 2, version 2.1-0*; Bruker AXS; Madison, WI, 2003−2004.
(26) *SHELXTL, version 6.12*; Bruker AXS; Madison, WI, 2001.

exception of those involved in agostic bonding, whose positions were refined freely. All hydrogen atoms were assigned fixed isotropic thermal parameters calculated as $U_{iso}(H) = 1.2 \times U_{iso}(parent)$.

Single crystals of **1b**, **2**, and **3** suitable for X-ray diffraction analysis were grown via slow diffusion of CH_2Cl_2/C_6H_6 solutions and petroleum ether. Compound **1b** co-crystallized with two molecules of CH_2Cl_2 in the asymmetric fraction of the unit cell. One of these molecules was disordered about a 2-fold axis passing through both chlorine atoms, leading to a 64:36 occupancy ratio for the two alternate orientations. Each molecule of **2** co-crystallized with one-half molecule of C_6H_6 as solvate in the asymmetric unit.

Acknowledgment. We thank the Robert A. Welch Foundation for support (Grant No. AA-0006). The Bruker-Nonius X8 APEX diffractometer was purchased with funds received from the National Science Foundation Major Instrumentation Program (Grant No. CHE-0321214).

Supporting Information Available: Full details of the crystal structure analyses in CIF format, including data for compound **4**. This material is available free of charge via the Internet at http://pubs.acs.org.

IC700746J